

cylinders. The lengths of the several cylinders were so adjusted that the envelope of the array was an ellipsoid of revolution. 104 thermocouples connected in series were constructed by joining adjacent rods alternately with short lengths of fine copper and constantan ribbon. The rods were affixed in the frame with wax in order to prevent breakage of the thermocouples, and this circumstance completely vitiated Ellwood's results. The array was constructed at room temperature and experimented upon at a temperature somewhat higher, so that, in consequence of the differential thermal expansion of the specimen rods and frame, all the observations were made with the specimen material under stress. Accordingly the data give a better indication of the magnetostrictive behavior of the material than of its magneto-caloric behavior.<sup>9</sup> The specimen of carbon steel used in the present research was removed from Ellwood's assembly.

Agnes Townsend<sup>4</sup> has published a detailed description of the magneto-caloric effect at low fields in 1 mm rods of cold drawn nickel, and her data are in complete accord with those given in Table II above. It should be noted, however,

<sup>9</sup> The senior author of the present paper was responsible for the failure to detect this error at the time the work was done. The same fault appears in some early work on nickel of Agnes Townsend (Phys. Rev. 40, 120 (1932)). Credit is due Dr. Townsend not only for discovering the error, but for devising an experimental method which eliminates it.

that in the case of *annealed* materials the constraint imposed on the specimen by Dr. Townsend's method for attaching the thermocouples is sufficient completely to mask the true magneto-caloric behavior of the material. It is for this reason that the specimen mounting herein described was devised.

By far the most extensive research in this field is due to Okamura,<sup>10</sup> who worked with iron, nickel, cobalt, various carbon steels, piano wire, K.S. magnet steel, and iron-nickel alloy. Unfortunate flaws in his experimental method, however, prevent any quantitative comparison of his with the present data. For example, in iron, nickel and 0.2 percent carbon steel Okamura found no agreement whatever between the values of the hysteresis loss per half cycle as calculated from his magnetic and calorimetric measurements. Qualitatively, however, Okamura's results are similar to those given here except in the case of annealed iron, for which he found an initial heating on demagnetization instead of the cooling here reported.

In conclusion the authors desire to acknowledge with thanks the assistance of Dr. Agnes Townsend and Mr. R. J. Walsh during the early stages of the work, and of Dr. H. J. Glaubitz, who aided in the preparation of the data for publication.

<sup>10</sup> Okamura, The 363rd Report of the Research Institute for Iron, Steel, and Other Metals.

## The Ultrasonic Radiation Field of a Quartz Disk Radiating into Liquid Media

FRANCIS E. FOX AND GEORGE D. ROCK  
Catholic University of America, Washington, D. C.

(Received May 25, 1938)

The radiation pressure of sound waves on a spherical obstacle is used to determine the distribution of intensity in the sound field of a quartz disk radiating into a liquid medium. The measured distribution of intensity along the axis normal to a crystal face is compared to that to be expected from a plane piston radiating into a semi-infinite medium, and the agreement shows that the theoretical assumptions are fulfilled for the case used and that the "effective area" of the piston is essentially the actual area of the quartz disk.

### INTRODUCTION

INVESTIGATIONS conducted with quartz oscillators, or quartz resonators vibrating in gaseous media, have shown that the vibration is

very complicated. The face of an X cut resonator maintained at resonance for its fundamental longitudinal mode of vibration exhibits areas both of vigorous motion and comparative rest

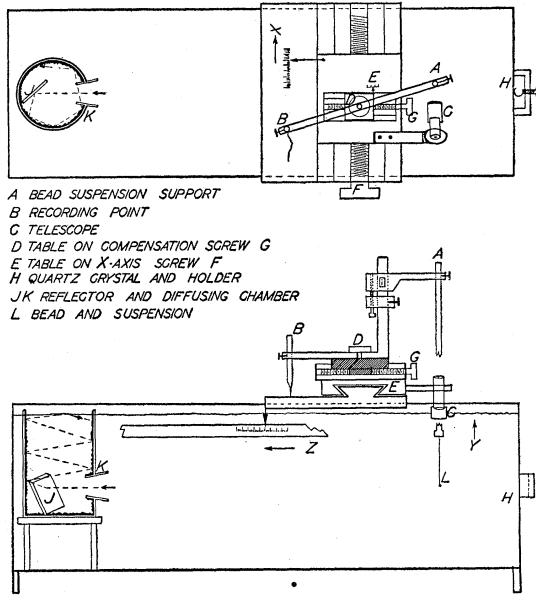


FIG. 1. Top and side view of tank and carriage.

when examined for nodes either by optical methods or by dusting with lycopodium powder. The extremely small damping in such resonators is responsible for their enormously high resonance amplitudes compared to the static piezoelectric change of dimensions with the driving voltages and makes the amplitude at resonance very sensitive to extremely small variations in the static dimensions of the resonator. At frequencies in the range of several megacycles a variation of thickness of less than a wave-length of visible light is enough to destroy resonance conditions for different parts of the crystal and in these parts the amplitudes fall to a small fraction of the values they would have at resonance. The driving voltage selects those sections of the crystal having dimensions corresponding to resonance and builds up the resonance amplitude, while those portions of the crystal for which the true resonance frequency would be even slightly different from the driving frequency remain comparatively at rest, having little more than the amplitude corresponding to the static deformation to be expected from the driving voltage. If the damping is larger, or if the frequency of the driving voltage does not correspond to exact resonance for any portion of the crystal, the amplitude for slightly different dimensions, al-

though very small compared to resonance amplitudes when vibrating in gases, might be much more uniform. In liquid interferometry the sound source is usually a quartz resonator with at least one side exposed to the liquid, so that the damping of the crystal is much larger than would be the case in air, the resonance amplitudes are correspondingly reduced, and it is possible that the vibration of the resonator is more uniform so that with a sound source radiating into liquid media the assumption of a "piston-like" motion of the source is justified.

#### METHOD OF INVESTIGATION

It was decided to investigate the distribution of intensity in an acoustic radiation field of such a source in order to see how well this assumption is fulfilled. The sound detector chosen utilizes the acoustic radiation pressure on a small sphere placed in the sound beam. Preliminary work had shown that with a horizontal sound beam of the intensity available, a small sphere suspended on an extremely fine quartz fiber 10-12 cm long could be deflected several centimeters from its rest position by the radiation pressure. While the driving frequency and power input to a quartz crystal radiating into a large trough was maintained constant the intensity distribution was measured by the deflection of the pendulum in various portions of the ultrasonic beam.

#### APPARATUS

The crystal was a circular X cut quartz disk of 1 cm radius mounted at a nodal plane for its fundamental resonance frequency, which is approximately 2.67 megacycles. The driving voltage was supplied by a transfer tuned *LC* circuit from a crystal-controlled oscillator at 2.49 megacycles. The current in the lead to the quartz was main-

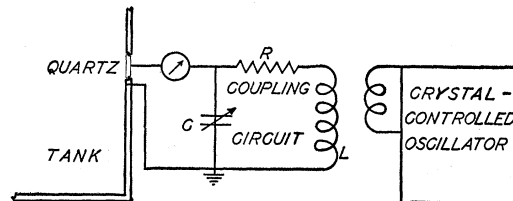


FIG. 2. Arrangement of associated apparatus.

apparatus is shown in Figs. 1 and 2. The sound source was set in the center of one end of a trough  $3 \times 1 \times 1$  feet with polished plate glass sides and bottom and hard rubber ends. A small lead sphere was attached to the support (*A*) by means of a fine quartz suspension. The support was an arm of a large vernier caliper with micrometer adjustment, so that the sphere could be raised or lowered in the sound beam (*Y* direction). To the lower end of the vernier caliper a recording stylus or pencil was attached, and the whole mounted on a table (*D*) which can be moved by a micrometer screw along the length of the trough (*Z* direction) to compensate for an observed deflection of the pendulum from the vertical. The micrometer screw was itself on a movable table (*E*) having another micrometer screw for motion across the trough (*X* direction) set in a large carriage which could be moved along the length of the trough (*Z* direction). The center of the coordinate system is taken as the center of the crystal face exposed to the liquid. In making the measurements the carriage was moved to the desired value of *Z*, the bead adjusted to the desired *Y*, and then the screw drive used to move the sphere from one side of the trough to the other along the *X* direction. As the pendulum is deflected, the bead is brought back to its original *Z* position by the compensating micrometer screw. To keep *Z* constant and compensate for the deflections that occur the image of the bead is focused on the cross hairs of a telescope mounted on table *E* so that as the deflections occur and the bead image is displaced it can be restored to its original position by means of the compensating screw. The recorder then traces a curve of *X* versus the "compensating distance" for constant values of *Y* and *Z*. The "compensation distance" of course is the deflection of the bead at the point *XYZ* in question.

Several difficulties arose in insuring the return of the bead to its original *Z* distance as the (*XD*) plot was traced. These were caused principally by the bead's moving out of focus if viewed from a stationary telescope pointing along the *X* axis, while if the telescope were mounted on the table *E* which moved in the *X* direction the bead had to be focused through a water-air boundary and due to slight waves on the water surface the

image continually flickered. The difficulty was finally overcome by placing a waterproof tube on the telescope with a plane glass window cemented on the end underneath the water level. Surface waves were then no disturbing factor and as the telescope accompanied the bead in the *X* direction the latter remained constantly in sharp focus at the cross hairs except for the deflection. Another difficulty was that of keeping the bead from being deflected in the *X* direction when intensity variations were rapid in that direction. The suspension was finally made bifilar, and spread to a separation of about 4 or 5 cm at the top. In the measurements given here the sphere was made of lead to cut down the large deflections obtained with lighter materials and to render unnecessary any compensation for the lift of the bead with deflections. The error in the *Y* position due to a small deflection *D* of a pendulum *L* cm long is  $\Delta Y \sim D^2/L$ . This error for the suspension used is less than 0.2 mm for the greatest deflection measured. The use of the heavy lead sphere also obviates the effects of the motion of the water. This was evident from the observations of the bead immediately after turning off the sound beam, since the deflection fell quickly to zero even though it was possible to detect by other means (e.g., the motion of small particles suspended in the water) a flow in the liquid in the direction of the sound beam. By using a very light bead the deflection due to this flow could be detected, and persevered for some seconds after the extinction of the sound beam. A further check was the insertion of a very thin collodion film (not thicker than several wavelengths of visible light) in front of the sphere. This prevented the water flow past the bead but allowed the radiation to pass. During the measurements frequent checks were made by obtaining traces for the same *YZ* values over a period of a month. In all cases these traces were coincident within the accuracy of the measurements. The traces taken in moving across the trough were retraced by the reverse motion.

In the early measurements instability of the bead at some maximum deflection points indicated the presence of standing wave systems in the trough, and attempts to line the trough with absorbing materials were not successful. When materials such as spongy rubber pads were first

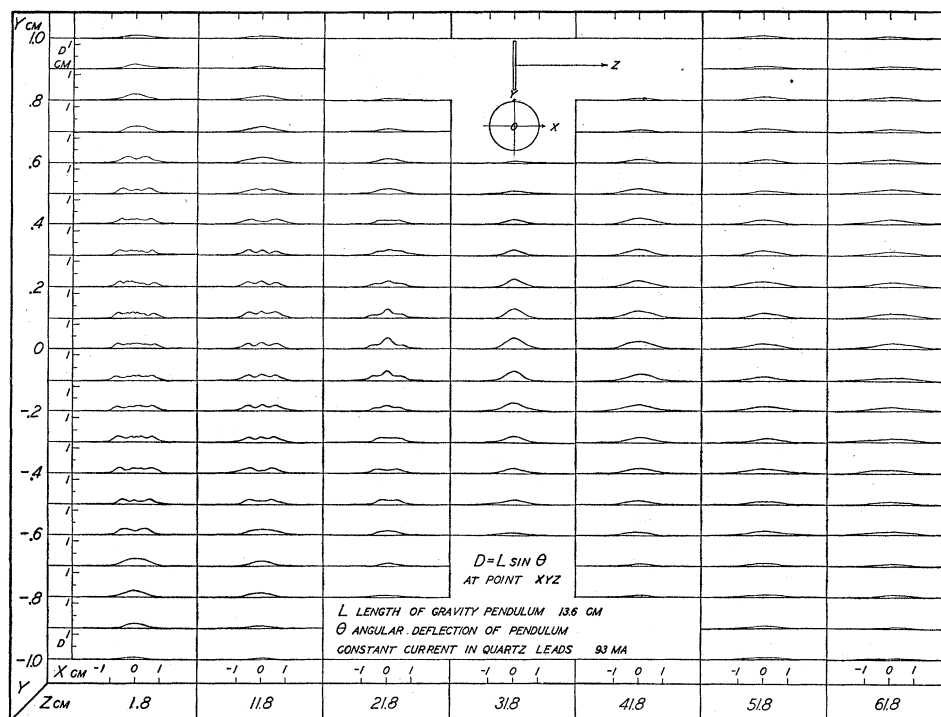


FIG. 3. Deflection along the X axis at constant values of Z and Y. Length of suspension 13.6 cm; mass of lead sphere 0.025 g; radius of sphere 0.081 cm; current in leads to quartz resonator 93 milliamperes.

used, the standing wave systems disappeared; but as the materials became wetted the absorption or diffuse scattering was almost negligible, transmission occurring through water soaked in the rubber almost as well as if the rubber were absent. A "diffuse scattering" and "absorbing" body was then constructed by analogy to the "black-body absorber" used in optics. The beam of sound was transmitted into a large cylinder 20 cm long and 15 cm diameter, through a slightly funnel-shaped opening in the side 6.5 cm wide; the sound beam was at most 4 cm wide at the far end of the trough. Inside was an oblique reflector which directed the reflected waves sideways and upwards so that they strike the container walls at a small angle and make many reflections on a single trip around the container, and because of their upward deflection continue to travel in a helical path to the top of the container where they are reflected downward again. The inside walls of the container were made to assist diffuse reflection, by coating them with a coarse gravel of irregular shape larger than the

wave-length of the radiation in the medium, so that the energy entering the container as coherent sound radiation is almost completely diffused and to some extent absorbed in the container. In fact after the sound had been streaming into the container for some time a slight flow of the water around the inside walls could easily be seen—the flow proceeding in the direction of the sound waves. Even with this device the standing wave system did not entirely disappear, but could be detected probably because the first reflector still transmitted a fair portion of the radiation which passed on to the walls and was reflected directly back to form a fairly easily detected standing wave system. Finally the container was made double-walled with an air space completely surrounding the inside cylinder and the reflector made of a prism of brass filled with air to decrease the direct transmission, since the over-all coefficient of transmission at an air-water boundary is several orders smaller than that at a metal-water boundary. In this form the device eliminated

any regular standing wave system that could be detected by either mechanical or optical means and the stability of the bead was all that could be desired.

MEASUREMENTS

In Fig. 3 traces are given for the values of  $Z$  and  $Y$  indicated. These give for a fixed distance the  $X$  versus  $D$  trace of the intensity distribution for values of  $Y$  one mm apart, and afford for each  $Z$  distance chosen a picture of fairly symmetrical distribution of intensity in the  $XY$  plane. The regular development of the traces taken at  $Y=0$  for increasing values of  $Z$  is more strikingly shown in Fig. 4 where the traces for  $Y=0$  (i.e., along the horizontal diameter of the crystal) were taken at intervals of 1 cm along the  $Z$  axis until at large value of  $Z$  the traces become very similar and larger intervals are used as indicated. In the region where the intensity was changing rapidly with  $Z$ , traces were made every half-cm, and although not included in the figures, measurements from these traces were used together with those in Fig. 5 to compare the experimental results with the theoretical intensity distribution along the  $Z$  axis.

THEORETICAL DISTRIBUTION OF INTENSITY ALONG THE  $Z$  AXIS

The exact expression for the distribution of intensity along the  $Z$  axis is easily obtained for a plane piston radiating into a semi-infinite medium. Crandall<sup>1</sup> gives the particle velocity potential along the  $Z$  axis of such a piston with radius  $R=m\lambda$ , where  $m$  is some constant and  $\lambda$  is the wave-length of sound as

$$\phi = -(\xi_0/k) \{ \sin [\omega t - k(Z^2 + m^2\lambda^2)^{\frac{1}{2}}] - \sin (\omega t - kZ) \}. \quad (1)$$

Here the velocity at the piston face is  $\xi_0 \cos \omega t$ , and  $k=2\pi/\lambda$  or  $\omega/c$  where  $\omega$  is  $2\pi$  times the frequency, and  $c$  is the velocity of sound. One can then expand, as Crandall does, the radical for values of  $Z > 3R$  but since the exact expression is of interest this need not be done. The ex-

pression can be written:

$$\phi = (2\xi_0/k) \{ \sin \frac{1}{2}k[(Z^2 + R^2)^{\frac{1}{2}} - Z] \times \cos \frac{1}{2}[2\omega t - k(Z^2 + R^2)^{\frac{1}{2}} - kZ] \}, \quad (2)$$

which yields for the maximum pressure

$$p_{\max} = \rho \phi_{\max} = 2\rho c \xi_0 \sin \pi[(Z^2 + R^2)^{\frac{1}{2}} - Z]/\lambda \quad (3)$$

and for the intensity

$$I = p_{\max}^2/2\rho c = 2\rho c \xi_0^2 \sin^2 \pi[(Z^2 + R^2)^{\frac{1}{2}} - Z]/\lambda. \quad (4)$$

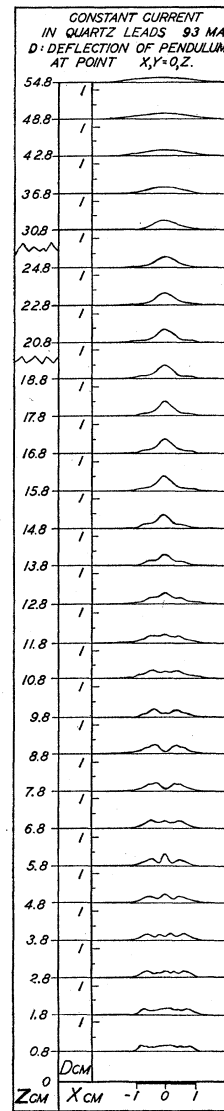


FIG. 4. Deflection along  $X$  axis for  $Y=0$  and  $Z$  as indicated. The scale factor is changed at  $Z=20$  and  $25$  cm to show the traces at large values of  $Z$ .

<sup>1</sup> Crandall, *Theory of Vibrating Systems and Sound* (Van Nostrand, 1926) p. 134. See also A. H. Davis, *Modern Acoustics* (Macmillan, N. Y., 1934) p. 61.

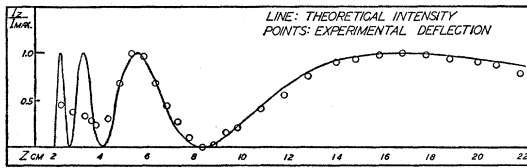


FIG. 5. Distribution of intensity along  $Z$  axis. The line is the theoretical distribution given by Eq (4) for  $\lambda=0.06$  cm;  $R=1.00$  cm; and  $2\rho c\xi_0^2=1$ =maximum deflection of pendulum. The circles are experimental values from the ( $XD$ ) curves expressed as the ratio of the deflection at  $Z$  to the maximum deflection. The diameter of the circles represent the thickness of the line made by the recorder.

For  $Z > 3R$  this immediately becomes

$$I \sim 2\rho c\xi_0^2 \sin^2 \pi R^2/2\lambda Z$$

or 
$$I \sim 2\rho c\xi_0^2 \sin^2 \pi m^2\lambda/2Z. \quad (5)$$

The latter is the form given and discussed by Crandall. From (4) or (5) it is evident that for values of  $Z$  greater than  $m^2\lambda$  the intensity falls continuously as  $Z$  approaches  $\infty$ . For values of  $Z$  less than  $m^2\lambda$  the intensity according to (5) passes through successive maxima and minima for values of  $m^2\lambda/Z=2, 3, 4 \dots$  the oscillation becoming more and more rapid as  $Z$  approaches 0. Although (5) would indicate an infinite number of maxima and minima and an indeterminate value at  $Z=0$  it can be seen from (4) that the maxima and minima occur at those values of  $Z$  which make the expression  $2[(Z^2+R^2)^{1/2}-Z]/\lambda$  equal to integers and that the intensity at  $Z=0$  depends on the value of the constant  $R/\lambda$ . If we write  $R/\lambda=(n+C)$  where  $n$  is an integer and  $(n+C)=m$  as formerly defined it is evident that the intensity at  $Z=0$  may have any value from zero to a maximum. It is zero for  $C=0$  and a maximum for  $C=\frac{1}{2}$ , and has intermediate values for all other values of  $C$ . It is also evident from (4) that as  $Z$  varies from 0 to  $\infty$  the angle takes values from  $\pi R/\lambda$  to 0, or from  $(n+C)\pi$  to 0, yielding  $n$  minima, excluding the one at  $Z=\infty$ , and either  $n$  or  $n+1$  maxima depending on whether  $C$  is less than or greater than  $\frac{1}{2}$ .

#### COMPARISON OF EXPERIMENTAL DATA WITH THEORY

On the traces made the last maximum occurred at 16.8 cm, the next nearest minimum at 8.3 cm, and the next nearest maximum at 5.3 cm. Although these are clearly defined the exact positions might have occurred within one of the half-cm intervals. By use of these values for  $Z$  as those making  $m^2\lambda/Z$  equal successively to 1, 2, 3 in (5) the computed values of  $R=m\lambda$  are 1.01, 1.00, and 0.98. The value of  $\lambda(0.06$  cm) was computed from the known velocity of sound in water and the frequency used. The agreement of the computed values of  $R$  with the measured radius of one cm is as good as could be expected from the method of determining the  $Z$  values used.

We assumed the value of 1 cm for  $R$  and used the value of  $\lambda$  as before and plotted the theoretical intensity distribution for values of  $Z$  from 2 to 22 cm, the maximum fitted to the value of the maximum deflection. The observed deflections along the  $Z$  axis were then plotted as ratios of the deflections at the point  $Z$  to the maximum deflection, and are shown in Fig. 5.

The radius of the circles used in marking the experimental points represents the accuracy of the experimental measurements so that again the agreement for large values of  $Z$  is all that could be expected. The lack of agreement for small values of  $Z$  is probably due to the fact that when the bead is near the crystal there are standing wave systems set up between the bead and the crystal which cannot be neglected, since the bead is not small in comparison with the wavelength. The use of a very small bead, so as both to increase the "resolving power" of the measuring device and minimize the effect of these standing wave systems, would undoubtedly enable one to secure better agreement for smaller values of  $Z$ .

The authors wish to acknowledge their indebtedness to Dr. Herzfeld of Catholic University, and Dr. Hubbard of Johns Hopkins University for many suggestions and discussions.